Numer. Math. Theor. Meth. Appl.
doi: 10.4208/nmtma.2011.y10013

Vol. **4**, No. 4, pp. 525-536
November 2011

Cubic Spiral Transition Matching G^2 Hermite End Conditions

Zulfiqar Habib[1,*] and Manabu Sakai[2]

[1] *COMSATS Institute of Information Technology, Department of Computer Science, Defense Road, Off Raiwind Road, Lahore, Pakistan.*
[2] *Department of Mathematics & Computer Science, Koorimoto 1-21-35, Kagoshima 890-0065, Japan.*

Received 25 June 2010; Accepted (in revised version) 6 April 2011

Available online 7 November 2011

Abstract. This paper explores the possibilities of very simple analysis on derivation of spiral regions for a single segment of cubic function matching positional, tangential, and curvature end conditions. Spirals are curves of monotone curvature with constant sign and have the potential advantage that the minimum and maximum curvature exists at their end points. Therefore, spirals are free from singularities, inflection points, and local curvature extrema. These properties make the study of spiral segments an interesting problem both in practical and aesthetic applications, like highway or railway designing or the path planning of non-holonomic mobile robots. Our main contribution is to simplify the procedure of existence methods while keeping it stable and providing flexile constraints for easy applications of spiral segments.

AMS subject classifications: 65D05, 65D07, 65D10, 65D17, 65D18

Key words: Path planning, spiral, cubic Bézier, G^2 Hermite, Computer-Aided Design (CAD), computational geometry.

1. Introduction

The research and development in the area of path planning include theoretical and practical aspects of geometric modeling approaches. Fair path planning is one of the fundamental problems, with numerous applications in the fields of science, engineering and technology such as highway or railway route designing, networks, robotics, GIS, navigation, CAD systems, collision detection and avoidance, animation, environmental design, communications, image processing, digital data compression, gear designing, and other disciplines [4, 15]. One of the main approaches to path planning is through the use of spline and spiral functions.

*Corresponding author. *Email addresses:* drzhabib@ciitlahore.edu.pk (Z. Habib), msakai@sci.kagoshima-u.ac.jp (M. Sakai)

In path planning it is often required to have a planar transition curve of J-shaped (between straight line and circle), U-shaped (between two straight lines), C-shaped (between two circles), and an S-shaped (between two circles) [6,7,9,18]. Planer spirals have monotonic curvature with constant sign, therefore such segments are free from singularities, inflection points, and curvature extrema. It is considered desirable to have such a curve in satellite path planning, highway or railway route designing, GIS, or non-holonomic (car-like) robot path planning [13,14]. In curve and surface design, it is mostly required to have a spiral curve of G^2 contact matching Hermite conditions, i.e., under the fixed positional, tangential, and curvature end conditions. These properties make spiral curves important for both physical [4] and aesthetic applications [1].

Dietz and Piper [2] have numerically computed values to aid in adjusting the selection of control points with the help of tables for building cubic spiral curve matching G^2 Hermite conditions. However, their numerically obtained spiral regions would become smaller or even empty as the tangent angles at end points become relatively equal. An extension of this method is discussed in [3] by using rational cubic function. Their method gives more spiral regions but the case of relatively equal tangent angles is not discussed. Further, another case of a very small tangent angle at start point leads to a spike near end point in their scheme.

Recently, Habib and Sakai [10] used rational cubic spline to find reachable regions for the spiral segment matching G^2 Hermite conditions. In their method, spiral conditions are derived on the whole segment by using derivative of curvature of polynomial. A free parameter is used to find the admissible region for a spiral segment with respect to the curvatures at its endpoints under the fixed positional and tangential end conditions. Although their method is stable and preserving all the geometric features to overcome the problems in [2, 3] but the analysis on finding the spiral regions is computationally very expensive (of degree 12 of derivative of curvature) due to the rational form of cubic polynomial.

This paper extends and simplifies the analysis of [2, 3, 8, 10, 16, 17] by using a single segment of cubic Bézier function for a C-shaped spiral segment matching G^2 Hermite end conditions. Our main contribution is the achievement of almost the same spiral regions by using a cubic polynomial in non-rational form. Computational cost of finding spiral regions is also very low because the degree of derivative of its curvature is just five (instead of twelve). Since spiral conditions are derived on the whole segment, our proposed method is stable and there is no fear of spiking phenomenon of non-monotone curvature.

2. Background

2.1. Notations and conventions

The usual Cartesian co-ordinate system is presumed. Boldface is used for points and vectors, e.g.,

$$\boldsymbol{a} = \begin{pmatrix} a_x \\ a_y \end{pmatrix}. \tag{2.1}$$

The Euclidean norm or length of a vector $\boldsymbol{a}$ is denoted by the notation

$$\|\boldsymbol{a}\| = \sqrt{a_x^2 + a_y^2}. \tag{2.2}$$

The positive angle of a vector $\boldsymbol{a}$ is the counter-clockwise angle from the vector $(1,0)$ to $\boldsymbol{a}$. The derivative of a function f is denoted by f'. To aid concise writing of mathematical expressions, the symbol $\times$ is used to denote the signed z-component of the usual three-dimensional cross-product of two vectors in the xy plane, e.g.

$$\boldsymbol{a} \times \boldsymbol{b} = a_x b_y - a_y b_x = \|\boldsymbol{a}\|\|\boldsymbol{b}\| \sin\theta, \tag{2.3}$$

where θ is the counterclockwise angle from $\boldsymbol{a}$ to $\boldsymbol{b}$. The signed curvature of a parametric curve $\boldsymbol{P}(t)$ in the plane is

$$\kappa(t) = \frac{\boldsymbol{P}'(t) \times \boldsymbol{P}''(t)}{\left\|\boldsymbol{P}'(t)\right\|^3}, \tag{2.4}$$

when $\|\boldsymbol{P}'(t)\|$ is non-zero. The derivative of curvature in (2.4) yields

$$\kappa'(t) = \frac{\phi(t)}{\left\|\boldsymbol{P}'(t)\right\|^5}, \tag{2.5}$$

where

$$\phi(t) = \|\boldsymbol{P}'(t)\|^2 \frac{\mathrm{d}}{\mathrm{d}t}\Big\{\boldsymbol{P}'(t) \times \boldsymbol{P}''(t)\Big\} - 3\Big\{\boldsymbol{P}'(t) \times \boldsymbol{P}''(t)\Big\}\Big\{\boldsymbol{P}'(t) \cdot \boldsymbol{P}''(t)\Big\}.$$

Descartes rule of signs ([12], pp. 439-443) is a technique for determining the number of positive or negative real roots of a polynomial. It is first described by Rene Descartes as "If the terms of a single-variable polynomial with real coefficients are ordered by descending variable exponent, then the number of positive roots of the polynomial is either equal to the number of sign differences between consecutive nonzero coefficients, or less than it by a multiple of 2."

The term 'spiral' refers to a curved line segment whose curvature varies monotonically with constant sign. In other words a curve segment with monotonically increasing curvature $\kappa(t)$ qualifies as a spiral if

$$\kappa(t) \geq 0, \quad \kappa'(t) \geq 0. \tag{2.6}$$

According to Kneser's theorem [5] any circle of curvature of a spiral arc contains every smaller circle of curvature of the arc in its interior and in its turn is contained in the interior of every circle of curvature of greater radius. So two distinct circles of curvature of a spiral arc never intersect and we cannot find the transition curve with a single spiral segment between two intersecting circles.

Conventional G^2 Hermite data are two points, unit vectors at those two points, and signed curvatures at those two points. A G^2 point of contact of two curves is a point where the two curves meet and where their unit tangent vectors and signed curvatures match.

3. Description of method

If a cubic spiral is to exist satisfying given positional, tangential, and curvature end conditions, necessarily, some cubic polynomial must exist which satisfies these end conditions, i.e., G^2 Hermite end conditions. Naturally the question arises whether or not it is without any internal curvature extrema. We first normalize the given data and then use Descartes rule of signs on derivative of curvature of cubic function to find sufficient conditions for the spiral curve.

A cubic Bézier curve has eight degrees of freedom in the interval $t \in [0,1]$, and is represented as

$$\boldsymbol{P}(t) = (1-t)^3\boldsymbol{p}_0 + 3t(1-t)^2\boldsymbol{p}_1 + 3t^2(1-t)\boldsymbol{p}_2 + t^3\boldsymbol{p}_3, \tag{3.1}$$

where $\boldsymbol{p}_i$, $i = 0,\cdots,3$, be the four distinct control points, shown as small disks in Fig. 1.

First we normalize the given G^2 Hermite data by transformation according to Fig. 1. We assume throughout this paper that the end points of Bézier spiral are $\boldsymbol{p_0}$ = (-1,0) and $\boldsymbol{p_3}$ = (1,0). As Bézier polynomials have affine invariance properties, this condition will not cause any loss of generality. Tangential end conditions for the cubic curve are represented as angles ϕ_0 and ϕ_1. As shown in Fig. 1, the tangent lines for the cubic curve at $t = 0$ and $t = 1$, and the horizontal axes form a triangle with angles ϕ_0 and ϕ_1 at the start and end points of curve respectively. Parametric spirals may be of increasing or decreasing curvature with the change of direction of parametrization. Without loss of generality, we can impose the condition on tangent angles: $0 < \phi_0 < \phi_1 < \pi/2$, for the cubic segment of increasing curvature for increasing values of parameter t.

As in [2], lengths of the lower left and right hand sides of the triangle in Fig. 1 are

$$d_0 = \frac{2\sin\phi_1}{\sin(\phi_0+\phi_1)}, \quad d_1 = \frac{2\sin\phi_0}{\sin(\phi_0+\phi_1)},$$

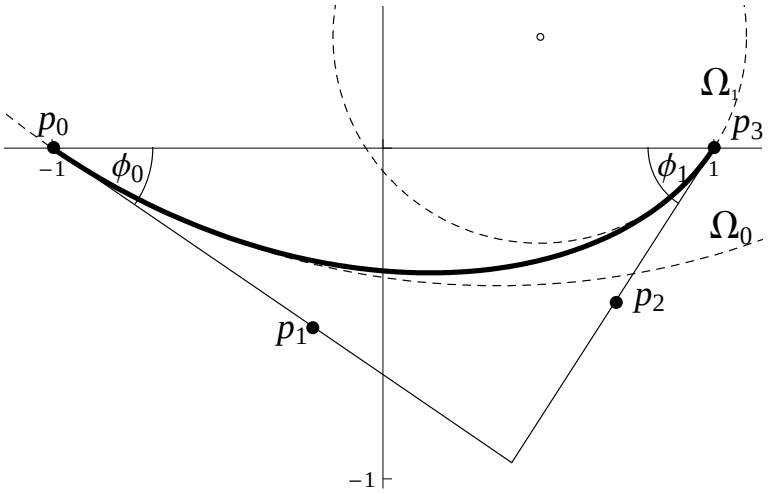

Figure 1: A cubic Bézier spiral transition between two circles with given end points, tangents, and curvatures.

respectively. Then the curvature end conditions are represented as $\kappa(0)$ and $\kappa(1)$ and are given in terms of the ratios

$$f_0 = \frac{\left\|\boldsymbol{P}'(0)\right\|}{d_0}, \qquad f_1 = \frac{\left\|\boldsymbol{P}'(1)\right\|}{d_1}. \tag{3.2}$$

Two control points $\boldsymbol{p}_1$ and $\boldsymbol{p}_2$ can be expressed in terms of f_0, f_1, ϕ_0, and ϕ_1 as

$$\boldsymbol{p_1} = \boldsymbol{p_0} + \frac{d_0 f_0}{3}(\cos\phi_0, -\sin\phi_0), \qquad \boldsymbol{p_2} = \boldsymbol{p_3} - \frac{d_1 f_1}{3}(\cos\phi_1, \sin\phi_1). \tag{3.3}$$

Therefore, from the formula of curvature in (2.4), the relations between parameters (f_0, f_1) and curvatures at end points (κ_0, κ_1) are given by

$$\kappa(0) = \frac{4(3-f_1)\sin\phi_0}{f_0^2 d_0^2}, \qquad \kappa(1) = \frac{4(3-f_0)\sin\phi_1}{f_1^2 d_1^2}. \tag{3.4}$$

Next we impose the spiral conditions to guarantee the absence of any internal curvature extremum in the transition curve defined in (3.1) on the whole segment, i.e., the derivative of curvature $\kappa'(t)$, defined in (2.5), has no zero on $[0,1]$. First spiral condition in (2.6) can be achieved if both f_0 and f_1 are constrained to be between 0 and 3, then the parametric cubic spiral will be free from inflection points. For convexity, this fact and the angle restriction are necessary [2]. For the second spiral condition in (2.6), first we introduce a new parameter s to simplify the condition $s \geq 0$ instead of $t \in [0,1]$. Therefore the derivative of curvature $\kappa'(t)$ (of degree 5 for our cubic case) for $t = 1/(1+s)$ yields

$$\left\|\boldsymbol{P}'(t)\right\|^5 \kappa'(t) = \frac{12 d_0 d_1}{(1+s)^5} \sum_{i=0}^{5} H_i(f_0, f_1; \phi_0, \phi_1) s^i, \tag{3.5}$$

where $H_i,\ i = 0, \cdots, 5$ are expressed in symmetric functions as

$$\begin{aligned}
H_0[f_0, f_1; \phi_0, \phi_1] &= f_1^2 d_1 \left\{ \left(9 - f_0^2 - 10 f_1 + 3 f_0 f_1\right) \sin\phi_0 + (f_0 - 3)^2 \sin(\phi_0 + 2\phi_1) \right\}, \\
H_1[f_0, f_1; \phi_0, \phi_1] &= 2 f_1 \Big[2 \sin\phi_0 \cos\phi_1 (f_0 - 3) \left(2 f_0^2 + 17 f_1 - 7 f_0 f_1 - 18\right) \\
&\qquad - \frac{d_1 \sin\phi_0}{2} \left\{ (f_0 - 3) \left(4 f_0^2 - 14 f_0 f_1\right) + f_1^2 (9 f_0 - 22) \right\} \\
&\qquad - 4 \cos\phi_0 \sin\phi_1 (f_0 - 3)^3 \Big], \\
H_2[f_0, f_1; \phi_0, \phi_1] &= 4 f_1 \Big[\sin\phi_0 \cos\phi_1 \left\{ 6(2 f_1 - 3) + f_0 (15 - 32 f_1) + f_0^2 (12 - 5 f_0 + 10 f_1) \right\} \\
&\qquad + \frac{d_1 \sin\phi_0}{2} \left\{ 5 f_0^3 - 2 f_1^2 - 2 f_0^2 (6 + 5 f_1) + f_0 f_1 (12 + 5 f_1) \right\} \\
&\qquad \cos\phi_0 \sin\phi_1 (f_0 - 3)^2 (5 f_0 - 2) \Big], \\
H_i[f_0, f_1; \phi_0, \phi_1] &= H_{5-i}[f_1, f_0; \phi_1, \phi_0], \qquad i = 3, 4, 5.
\end{aligned}$$

Since d_0, d_1, ϕ_0, and ϕ_1 come from the given G^1 part of the G^2 Hermite data (so are known), therefore two free parameters f_0, and f_1 allow us to match the given G^2 Hermite

data. For the spiral curve matching G^2 Hermite conditions, we need to find out the ranges of the ratios f_0 and f_1 (called spiral regions) for which the right hand side of expression in (3.5) remains non-negative, necessary to satisfy the second spiral condition in (2.6). Following theorem establishes the sufficient spiral condition on $(f_0, f_1, \phi_0, \phi_1)$.

Theorem 3.1. *A cubic Bézier curve of the form* (3.1) *is a spiral segment if*

$$H_i \geq 0 \ (i = 0, 2, 3, 5), \quad H_1 + 2\sqrt{H_0 H_2} \geq 0, \quad H_4 + 2\sqrt{H_3 H_5} \geq 0. \tag{3.6}$$

Proof. Due to the fact:

$$\begin{aligned} a + bx + cx^2 \geq & a + 2\sqrt{ac}x + cx^2, \\ & = \left(\sqrt{a} + \sqrt{c}x\right)^2. \end{aligned}$$

the conditions established in (3.6) are sufficient. □

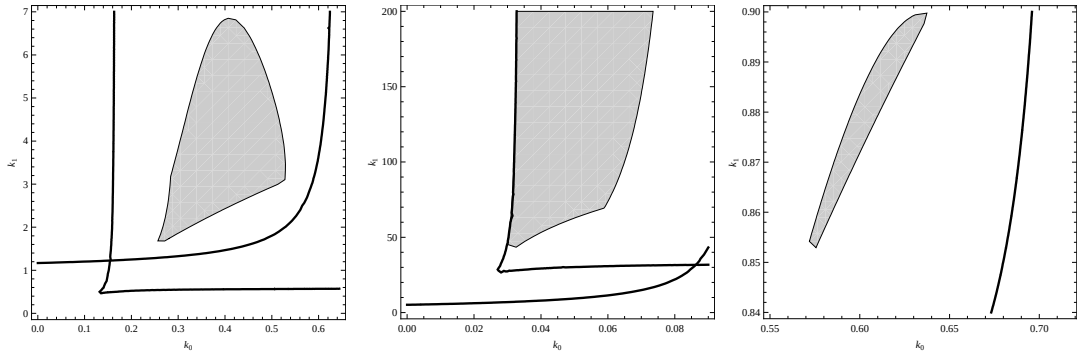

(a) $(\phi_0, \phi_1) = (0.7, 1.4)$ (b) $(\phi_0, \phi_1) = (0.1, 1.5)$ (c) $(\phi_0, \phi_1) = (0.8, 0.9)$

Figure 2: Spiral regions with respect to curvatures at the endpoints.

The algebraically simple parameters (f_0, f_1) do not give direct information on how to match or approximate given curvature values at the endpoints. We consider the problem of finding useful approximation to the admissible set of endpoint curvatures (κ_0, κ_1) for a cubic spiral curve under the fixed positional and tangential end conditions. Derivation of spiral regions in (κ_0, κ_1) curvature space is given in Appendix A for readers. Our approach is almost similar to the analysis for the rational cubic case discussed in [10].

Necessary conditions for cubic spirals can be obtained from the discriminant of $g(f_0)$ in (A.4) and the fact that the osculating circle at the endpoint $\boldsymbol{p}_3$ is completely inside the osculating circle at the start point $\boldsymbol{p}_0$. These conditions are discussed in [2, 3, 10], and provide lower boundaries of the region in which any spiral segment may be achieved. These boundaries are shown by dark solid hyperbolas in Fig. 2.

3.1. Numerical determination of spiral regions

In this section some numerical examples, with given tangent angles are considered for the spiral regions with respect to curvatures at the endpoints. These spiral regions are

shown in Fig. 2 with the gray shades. We have considered the following cases.

Case 1. $(\phi_0, \phi_1) = (0.7, 1.4)$: Spiral region is shown in Fig. 2(a).

Case 2. $(\phi_0, \phi_1) = (0.1, 1.5)$: This is the case when the tangent angle at start point becomes very small. As a result curvature at start point also becomes very small. Spiral region is shown in Fig. 2(b).

Case 3. $(\phi_0, \phi_1) = (0.8, 0.9)$: This special case occurs when the tangent angle at start point is slightly less than the tangent angle at endpoint. As a result curvature at start point also becomes slightly less than the curvature at endpoint. Spiral region is shown in Fig. 2(c).

3.2. The algorithm

Based on the above analysis, we have proposed a method to construct a G^2 Hermite cubic Bézier spiral with a single segment. It is described in the following algorithm:

1. Given are endpoints, tangent directions and curvatures at endpoints.
2. Normalize the endpoints by transformation according to Fig. 1.
3. Find f_0, f_1 from (A.10) and (A.2), respectively.
4. Find the spiral regions from the conditions in (3.6) and (A.9).
5. If given end curvatures does not belong to the spiral region then go to the first step for other suitable combination of tangent directions and curvatures at endpoints.
6. Find the required spiral segment from (3.1) and (3.3).
7. Apply the reverse transformation to bring the spiral transition curve back to its original location.

4. Numerical examples

We consider the following examples of G^2 Hermite cubic Bézier spiral transitions. Their corresponding curvature plots and derivative of curvature plots are given in Fig. 3 as a verification of our claim. Data of these examples is in normalized Hermite form. As before, the endpoints of spiral segment are fixed at $\boldsymbol{p_0} = (-1, 0)$ and $\boldsymbol{p_3} = (1, 0)$, the tangent angles and curvatures at endpoints are (ϕ_0, ϕ_1) and (κ_0, κ_1), respectively.

Example 1. For $(\phi_0, \phi_1) = (0.7, 1.4)$ and $(\kappa_0, \kappa_1) = (0.4, 4)$. Figs. 3(a)-3(c) give illustrations of case 1 (Fig. 2(a)).

Example 2. For $(\phi_0, \phi_1) = (0.1, 1.5)$ and $(\kappa_0, \kappa_1) = (0.035, 100)$. Figs. 3(d)-3(f) describe the special case 2 (Fig. 2(b)). In this example, curvature at start point is very small as compared to curvature at the endpoint.

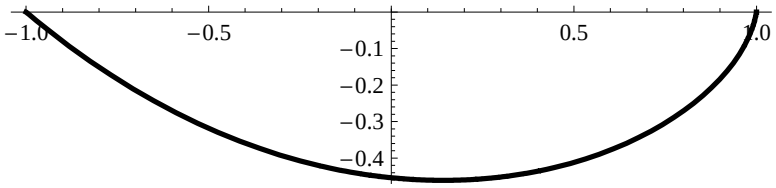

(a) A simple spiral curve with $(\phi_0, \phi_1) = (0.7, 1.4)$, $(\kappa_0, \kappa_1) = (0.4, 4)$

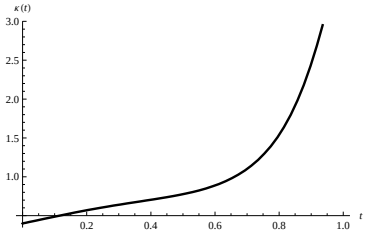

(b) Curvature plot

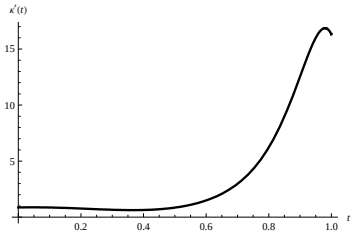

(c) Derivative of curvature plot

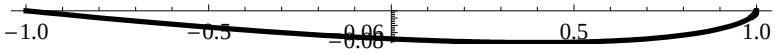

(d) A special spiral curve with $(\phi_0, \phi_1) = (0.1, 1.5)$, $(\kappa_0, \kappa_1) = (0.035, 100)$

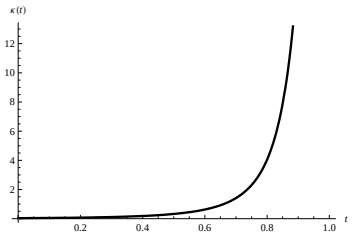

(e) Curvature plot

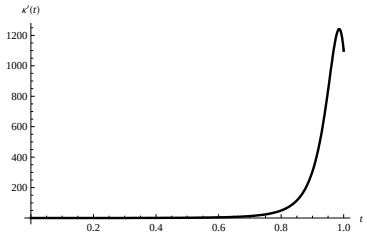

(f) Derivative of curvature plot

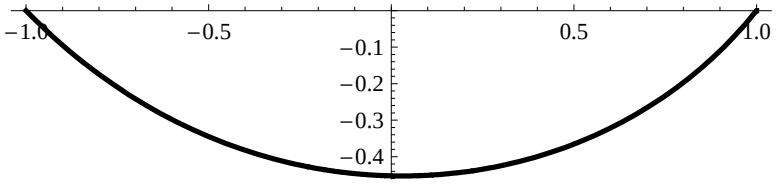

(g) A special spiral curve with $(\phi_0, \phi_1) = (0.8, 0.9)$, $(\kappa_0, \kappa_1) = (0.6, 0.874)$

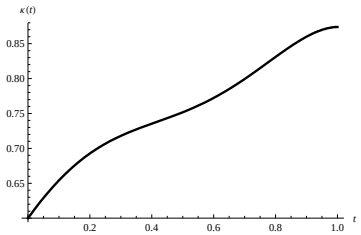

(h) Curvature plot

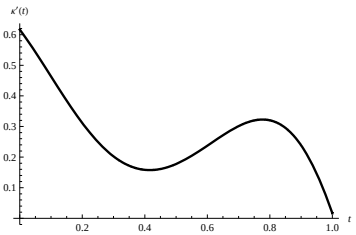

(i) Derivative of curvature plot

Figure 3: G^2 Hermite cubic Bézier spiral curves.

Example 3. For $(\phi_0, \phi_1) = (0.8, 0.9)$ and $(\kappa_0, \kappa_1) = (0.6, 0.874)$. Figs. 3(g)-3(i) deal with case 3 (Fig. 2(c)), when curvatures at the endpoints are almost equal.

We have explored the possibilities of more simple analysis on finding the spiral regions for a single segment of cubic spline interpolation matching positional, tangential, and curvature end conditions. Our algorithm also handles the special cases successfully. For example, when the curvature at start point is much less than the curvature at endpoint. Spiral regions with respect to curvatures at the endpoints are shown as gray shade in Fig. 2(b). Similar case with same spiral region is highlighted in Fig. 7 of [3] by using rational cubic Bézier function. The difference in the range of curvatures is due to the same as in the scaling of normalized data described by Fig. 1 of this paper and that of [3]. In some cases rational cubic function used in [3,10] may provide slightly larger spiral regions but this is achieved at the cost of higher computation than using a simple cubic function in (3.1).

Another special case when curvature at start point is slightly less than the curvature at endpoint, or when curvatures at both endpoints are almost equal. The spiral regions for such cases are not easy to visually detect and NVR (Non-viable region) is marked in Table 1 of [2]. An example of this case is given in Fig. 2(c) for $(\phi_0, \phi_1) = (0.8, 0.9)$ used in conjunction with $(\kappa_0, \kappa_1) = (0.6, 0.874)$ in Figs. 3(g)–3(i). Any example similar to this case is not given in [2,3].

Most of the discussion in Sections 3, 4 and 5 of [3] is on the procedure of formulating the problem of optimization of rational cubic spiral, discretization, and stability issues. The possibilities of hidden curvature extrema are minimized but could not be removed due to the analysis on discrete values of $t \in [0,1]$. Our procedure of derivation of spiral regions and finding the range of a free parameter for the spiral segment is significantly simplified due to the evaluation of the derivative of the curvature for real values of $t \in [0,1]$. Spiral conditions are computationally stable and derived on the whole segment.

Future work along this direction can be continued along various directions. For example the condition established by test is only sufficient condition and work can be done to find necessary condition for cubic Bézier spiral segments fitting Hermite conditions. Secondly, the condition of the test may be further relaxed to allow for greater flexibility by using Sylvester resultant. Finally, spiral curve matching G^2 Hermite end conditions could also be tried by using PH (Pythagorean hodograph) quintic function, introduced in [6,7,9,11,19], to explore the possibilities of more larger spiral regions to allow designers a comfortable range of end tangent directions and curvatures selections. However it will increase computational cost of derivation of conditions and execution of function.

Acknowledgments The authors are grateful to the editor and anonymous referees for their valuable comments and suggestions which have helped us to improve the presentation of this paper significantly. This work is partially supported by Kagoshima University of Japan.

A. Appendix

For given end tangents and end curvature conditions, i.e., for each quadruple $(\phi_0, \phi_1, \kappa_0, \kappa_1)$, values of f_0 and f_1 are sought so that the system of equations in (3.4) is satisfied, and the resulting cubic function (3.1) is a spiral. To simplify the analysis, we assume

$$e_0 = \frac{4\sin\phi_1}{d_1^2}, \quad e_1 = \left(\frac{\sin\phi_0}{\sin\phi_1}\right)^3. \tag{A.1}$$

Then first equation of (3.4) implies

$$f_1 = 3 - \frac{\kappa_0 f_0^2}{e_0 e_1}, \tag{A.2}$$

converting the second equation of (3.4) into monic quartic form $g(f_0) = 0$, such that

$$g(f_0) = f_0^4 - c_2 f_0^2 + c_1 f_0 + c_0, \tag{A.3}$$

where

$$c_0 = \frac{9e_0^2 e_1^2}{\kappa_0^2 \kappa_1}\left(\kappa_1 - \frac{e_0}{3}\right), \quad c_1 = \frac{e_0^3 e_1^2}{\kappa_0^2 \kappa_1}, \quad \text{and} \quad c_2 = \frac{6e_0 e_1}{\kappa_0}$$

are all positive for $\kappa_1 > e_0/3$ which leads to a lower bound on κ_1.

Next we need to find the positive real solution of $g(f_0)$. For this, its discriminant

$$D = \frac{1}{27}\left(4\lambda^3 - \mu^2\right) \tag{A.4}$$

should be non-negative, where

$$\lambda = 12c_0 + c_2^2, \quad \mu = 27c_1^2 + 72c_0c_2 - 2c_2^3. \tag{A.5}$$

Further, $g(f_0)$ can be factorized as

$$g(f_0) = (f_0^2 + \sqrt{p}f_0 + q)(f_0^2 - \sqrt{p}f_0 + r), \tag{A.6}$$

where

$$r + q = p - c_2, \quad r - q = \frac{c_1}{\sqrt{p}}, \quad qr = c_0. \tag{A.7}$$

Hence we have

$$\text{(i)} \quad q = \frac{1}{2}\left(p - c_2 - \frac{c_1}{\sqrt{p}}\right), \tag{A.8a}$$

$$\text{(ii)} \quad r = \frac{1}{2}\left(p - c_2 + \frac{c_1}{\sqrt{p}}\right), \tag{A.8b}$$

$$\text{(iii)} \quad p^3 - 2c_2p^2 + \left(c_2^2 - 4c_0\right)p - c_1^2 = 0. \tag{A.8c}$$

Theorem A.1. *For the conditions*

$$D \geq 0, \quad \kappa_1 > \frac{e_0}{3}, \tag{A.9}$$

the system of equations in (3.4) *has a positive solution* (f_0, f_1)*, where*

$$f_0 = \frac{1}{2}\left(\sqrt{p} - \sqrt{p - 4r}\right) \tag{A.10}$$

and f_1 *is given by* (A.2)*. Then the conditions in Theorem* 3.1 *give the spiral regions in* (κ_0, κ_1) *curvature space.*

Proof. From all the discussion above, we conclude that the system of equations in (3.4) can be solved by finding a positive real solution of third equation in (A.8c). By Descartes rule of signs, the cubic equation (A.8c)(iii) has at least one positive root which is

$$p = \frac{1}{3}\left(2c_2 + \eta^{1/3} + \lambda\eta^{-1/3}\right), \tag{A.11}$$

where

$$\eta = \frac{1}{2}\left(\mu + \sqrt{\mu^2 - 4\lambda^3}\right), \tag{A.12}$$

for λ and μ given in (A.5). That p can be proved positive by considering $4\lambda^3 \geq \mu^2$, and therefore by assuming $\eta = ke^{i\theta}$, for $k = \lambda^{3/2}$, $\theta \in [0, \pi]$, and by obtaining

$$p = \frac{2}{3}\left(c_2 + \sqrt{\lambda}\cos\frac{\theta}{3}\right) > 0. \tag{A.13}$$

Since q and r are also positive by (A.7), first factor of (A.6) has no positive root while the second has exactly two positive roots

$$f_0 = \frac{1}{2}\left(\sqrt{p} \pm \sqrt{p - 4r}\right), \tag{A.14}$$

if $\kappa_1 > e_0/3$ and $4\lambda^3 \geq \mu^2$.

In addition, we have to show that, for f_1 to be positive, at least one of the positive f_0 must belongs to $(0, u)$ by (A.2). Since

$$g(f_0) = \frac{e_0^3 e_1^2}{\kappa_0^2 \kappa_1}\{(u-3) + (f_0 - u)\} + 4u^2(f_0 - u)^2 + 4u(f_0 - u)^3 + (f_0 - u)^4,$$

therefore f_1, by (A.2), is positive for (A.14) if $u > 3$ and for $f_0 = (\sqrt{p} - \sqrt{p - 4r})/2$ if $u \leq 3$. This completes the proof of theorem. □

References

[1] H.G. Burchard, J.A. Ayers, W.H. Frey, and N.S. Sapidis. *Designing fair curves and surfaces*, chapter Approximation with aesthetic constraints. 1993.

[2] D. A. Dietz and B. Piper. Interpolation with cubic spirals. *Computer Aided Geometric Design*, 21(2):165–180, 2004.

[3] D. A. Dietz, B. Piper, and E. Sebe. Rational cubic spirals. *Computer-Aided Design*, 40:3–12, 2008.

[4] G. M. Gibreel, S. M. Easa, Y. Hassan, and I. A. El-Dimeery. State of the art of highway geometric design consistency. *ASCE Journal of Transportation Engineering*, 125(4):305–313, 1999.

[5] H. Guggenheimer. *Differential Geometry*. McGraw-Hill, New York, 1963.

[6] Z. Habib and M. Sakai. G^2 Pythagorean hodograph quintic transition between two circles with shape control. *Computer Aided Geometric Design*, 24(5):252–266, 2007.

[7] Z. Habib and M. Sakai. On PH quintic spirals joining two circles with one circle inside the other. *Computer-Aided Design*, 39(2):125–132, 2007.

[8] Z. Habib and M. Sakai. Fair path planning with a single cubic spiral segment. pp.121–125, USA, August 2008. The Proceedings of IEEE International Conference on Computer Graphics, Imaging and Visualization, Malaysia, IEEE Computer Society Press.

[9] Z. Habib and M. Sakai. Transition between concentric or tangent circles with a single segment of G^2 PH quintic curve. *Computer Aided Geometric Design*, 25(4-5):247–257, 2008.

[10] Z. Habib and M. Sakai. Admissible regions for rational cubic spirals matching G^2 hermite data. *Computer-Aided Design*, 42(12):1117–1124, 2010.

[11] Z. Habib and M. Sakai. Interpolation with PH quintic spirals. USA, 2010. The Proceedings of IEEE International Conference on Computer Graphics, Imaging and Visualization, Sydney, IEEE Computer Society Press. In press.

[12] P. Henrici. *Applied and Computational Complex Analysis*, volume 1. Wiley, New York, 1988.

[13] A. Kelly and B. Nagy. Reactive nonholonomic trajectory generation via parametric optimal control. *The International Journal of Robotics Research*, 22(7/8):583–601, 2003.

[14] R. M. Murray, J. P. Laumond, and P. E. Jacobs. A motion planner for non-holonomic mobile robots. *IEEE Transactions on Robotics and Automation*, 10(3):577–593, 1994.

[15] K. Marjeta. Geometric hermite interpolation by cubic G^1 splines. *Nonlinear Analysis: Theory, Methods & Applications*, 70:2614–2626, 2009.

[16] A. A. Raza, Z. Habib, and M. Sakai. Interpolation with rational cubic spirals. pp.98–103, USA, October 2008. The Proceedings of 4th IEEE International Conference on Emerging Technologies, ICET-Pakistan, IEEE Computer Society Press.

[17] M. Sakai. Osculatory interpolation. *Computer Aided Geometric Design*, 18(8):739–750, 2001.

[18] D. Sarpono, Z. Habib, and M. Sakai. Fair cubic transition between two circles with one circle inside or tangent to the other. *Numerical Algorithms*, 51(4):461–476, 2009.

[19] D. J. Walton and D. S. Meek. G^2 curve design with a pair of Pythagorean hodograph quintic spiral segments. *Computer Aided Geometric Design*, 24(5):267–285, 2007.